Journal of Applied Polymer Science

Encapsulation of Magnetic Nickel Nanoparticles via Inverse Miniemulsion Polymerization

Ana Paula Romio,[1] Heloísa H. Rodrigues,[1] Augusto Peres,[2] Alexandre Da Cas Viegas,[3] Elena Kobitskaya,[4] Ulrich Ziener,[4] Katharina Landfester,[5] Claudia Sayer,[1] Pedro H. H. Araújo[1]

[1]Department of Chemical Engineering and Food Engineering, Federal University of Santa Catarina, Florianópolis, SC, Brazil
[2]Petrochemical Technology, CENPES/PETROBRAS, Rio de Janeiro, Brazil
[3]Department of Physics, Federal University of Santa Catarina, Florianópolis, SC, Brazil
[4]Institute of Organic Chemistry III – Macromolecular Chemistry and Organic Materials, University of Ulm, Ulm, Germany
[5]Max Planck Institute for Polymer Research – MPI-P, Mainz, Germany
Correspondence to: P. H. H. Araújo (E-mail: pedro@enq.ufsc.br)

ABSTRACT: In this work, the encapsulation of magnetic nickel nanoparticles in polyacrylamide particles was performed via inverse miniemulsion polymerization. The dispersion of nickel nanoparticles was characterized in polar solvents including water, ethanol, and dimethyl sulfoxide using different stabilizers. The best results were obtained when the nonionic stabilizer poly(ethylene glycol) octadecyl ether (Brij 76) was used to stabilize the nickel nanoparticles in dimethyl sulfoxide. In addition, the block copolymer poly(ethylene-*co*-butylene)-*b*-poly(ethylene oxide) was used as a surfactant to create inverse miniemulsions while minimizing the coalescence of the miniemulsion droplets. Different types of salts such as zinc, nickel, and sodium nitrates were tested as lipophobes to retard Ostwald ripening. Transmission electron microscopy images of polyacrylamide/nickel particles synthesized with zinc and nickel salts as lipophobes indicate that nickel nanoparticles are embedded in the polyacrylamide matrix. Magnetization curves show that the saturation magnetization of polyacrylamide/nickel particles is only slightly below that of the pure nickel nanoparticles. © 2012 Wiley Periodicals, Inc. J. Appl. Polym. Sci. 129: 1426–1433, 2013

KEYWORDS: nanoparticles; nanowires and nanocrystals; emulsion polymerization; composites

Received 28 September 2012; accepted 9 November 2012; published online 12 December 2012
DOI: 10.1002/app.38840

INTRODUCTION

Organic–inorganic magnetic nanoparticles synthesized by miniemulsion polymerization combine the advantages of polymer latexes, such as high solid content, low viscosity, good process control of polymer composition and functionality with the properties of inorganic magnetic nanoparticles.[1] Among those metallic nanoparticles, the ones formed by Co, Fe, and Ni had received considerable attention due to their unique magnetic properties.[2–6] Nickel nanoparticles, in particular, present great potential in many fields of application, including electromagnetic interference shielding,[4,7] catalysis[8] and electro-conductive materials.[9] Nevertheless, nickel nanoparticles have a strong tendency to aggregate and form large clusters, thus losing their specific magnetic properties and limiting their practical use.[10] This problem can be overcome by the encapsulation of the nickel nanoparticles with a polymer shell that could not only prevent aggregation but also provide nanoparticles with specific functionalities.

The encapsulation of hydrophilic inorganic nanoparticles by direct (oil in water) miniemulsion polymerization requires the modification of the nanoparticle surface to change its hydrophilic–hydrophobic character[11] as it is extremely difficult for hydrophilic inorganic nanoparticles to diffuse into nonpolar monomer droplets.[12] Transferring the encapsulation process to inverse miniemulsion polymerization, where the dispersed phase is a polar (water-soluble) monomer, could avoid the necessity of surface modification of the hydrophilic inorganic nanoparticles.

In the inverse miniemulsion, the polymerization occurs in submicrometric aqueous (polar) droplets containing a water-soluble monomer, such as hydroxyethyl methacrylate,[13] acrylamide[14] or acrylic acid,[15] and lipophobic osmotic pressure agents, usually a highly hydrophilic salt or low-molecular weight electrolyte, for instance, NaCl[13] and $MgSO_4$,[14] to minimize diffusional droplet degradation. The droplets are dispersed in a continuous organic media (nonpolar) with an oil-soluble non-ionic surfactant producing stable colloidal particles.[16,17] The polymerization can

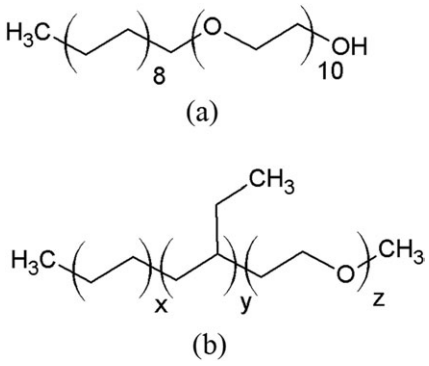

Figure 1. Chemical structures of the surfactants, (a) poly(ethylene glycol) octadecyl ether (Brij 76), (b) poly[(butylene-co-ethylene)-*b*-(ethylene oxide)] (PE/B-*b*-PEO).

be initiated by an initiator either from the droplet or the continuous phase.

Several works have been performed taking advantage of the solubility of salts in the monomer droplets of inverse miniemulsion polymerization in order to encapsulate the salts, such as zinc nitrate in polyacrylamide nanoparticles,[18] and to use the polar monomer droplets as nanoreactors, e.g., to perform the reduction of silver nitrate in silver nanoparticles via the polyol process and to process the subsequent polymerization of the *N*-vinylpyrrolidone present in the droplets.[19] The direct encapsulation of magnetic iron oxide nanoparticles with an average particle size around 10 nm in polyacrylamide,[20] poly(NIPAAm-*co*-MAA)[21] and poly(*N*-vinylcaprolactam)[22] via inverse miniemulsion polymerization was also performed demonstrating that the inverse miniemulsion polymerization is an effective way to synthesize magnetic polymeric particles.

Here, we report the encapsulation of nickel nanoparticles in a polyacrylamide matrix via inverse miniemulsion polymerization comparing the effect of different metal salts, including zinc, nickel and sodium nitrates used as lipophobes on the characteristics of the final particles. The morphology and the magnetic properties of the hybrid polyacrylamide/nickel particles were investigated by transmission electron microscopy and vibrating sample magnetometer analyses, respectively.

MATERIALS AND METHODS

Materials

Acrylamide (Acrylamide (Aldrich), Seelzen, Germany), used as monomer, was recrystallized from chloroform and vacuum dried at 25°C. The initiator, 2,2′-azoisobutyronitrile (AIBN, 98%, (Aldrich), Seelzen, Germany) was recrystallized from methanol and vacuum dried at 25°C. The block copolymer surfactant P(B/E-*b*-EO), consisting of a poly(ethylene-*co*-butylene)-*b*-poly(ethylene oxide) with a molecular weight of 5330 g mol^{-1} (PE/B-*b*-PEO; PE/B block: 4000 g mol^{-1}), was synthesized by anionic polymerization as described elsewhere.[23] The chemical structures of surfactants are shown in Figure 1.

All other chemicals were used as received. As solvents were employed either dimethyl sulfoxide (DMSO (Aldrich), Seelzen, Germany), ethanol (Aldrich), Seelzen, Germany or demineralized water. As lipophobes were used either nickel nitrate hexahydrate [$Ni(NO_3)_2{\cdot}6H_2O$, nickel nitrate (Strem), Kehl, germany, 99.0%], zinc nitrate hexahydrate [$Zn(NO_3)_2{\cdot}6H_2O$, zinc nitrate (Fluka), Buchs, Switzerland, 99.0%] or sodium nitrate ($NaNO_3$, Aldrich, 99.0%). The Nickel nanoparticles (NaBond), Shenzhen, China, (Ni, 99.9%) were obtained from NaBond Technologies Co. The stabilizers for the Ni NPs were poly(ethylene glycol) octadecyl ether (Brij 76 (Aldrich), Seelzen, Germany), ethoxylates of alkyl poly(ethylene glycol ethers) (Lutensol AT11 and Lutensol AT50, Lutensol (BASF), Ludwigshafen, Germany), polyoxyethylene sorbitan monooleate (Tween 80 (Oxiteno), Suzano, Brasil) or sodium lauryl sulfate (SDS (Aldrich), Seelzen, Germany). Isopar M (Exxon Mobil), Hamburg, Germany), a mixture of branched saturated hydrocarbons with an average chain length close to 12.5, was used as continuous phase. Toluene and acetone (Merck), Darmstadt, Germany were obtained from Merck.

Synthesis of Magnetic Polymeric Particles

In order to prepare the polar phase, Ni NPs were dispersed with a sonifier (W450 Digital, Branson, 1/4" tip) at 70% amplitude for 15 min of pulsed sonication (on/off time 25 s/10 s) in a DMSO containing 2.06 wt % Brij 76 solution prepared previously by magnetic stirring. Afterwards, AAm and the respective salt were added and the dispersion was prepared by sonication (W450 Digital, Branson, 1/4" tip) at 70% amplitude for 2 min. The nonpolar phase was prepared by dissolution of the surfactant PE/B-*b*-PEO in Isopar M at 60°C and then was added to the polar dispersion under stirring. After 1-hour of mechanical stirring the miniemulsion was prepared by sonication for 240 s at 70% amplitude. To prevent the premature start of polymerization, the miniemulsion was ice-cooled during the sonication. After this, the miniemulsion was purged with argon for 30 min under mechanical stirring (150 rpm). In order to carry out the polymerization, the temperature of the reaction mixture was increased to 65°C using an oil bath, and an oil-soluble initiator, AIBN dissolved in toluene, was added. The formulation for the preparation of the magnetic polymeric nanoparticles is given in Table I.

Characterization

Transmission electron microscopy (TEM) was performed with a Philips EM 400 electron microscope operating at 80 kV. The final latex was diluted with Isopar M and then dropped onto a 400 mesh carbon-coated copper grid and vacuum dried at 30°C. No further contrasting was applied. Field emission gun scanning electron microscopy (FEG-SEM) was performed with a JEOL, model JSM–6701F microscope, coupled to an energy dispersive system (EDS) microprobe. The samples were dried in an oven at 60°C for 12 h and sputter-coated with gold films. The particles were measured by image analysis (SizeMeter®) using the TEM images and then the particle size distribution and the number (Dp_n) and weight (Dp_w) average particle sizes, as well as the polydispersity index (PDI = Dp_w/Dp_n) were calculated. Statistical analysis was performed with at least 200 particles. The magnetic properties of Ni nanoparticles and PAAm/Ni particles were measured at 300 K using a 3473-70 Electromagnet vibrating sample magnetometer.

RESULTS AND DISCUSSION

Dispersion of Nickel Nanoparticles in the Polar Phase

A TEM image and the particle size distribution (PSD) of Ni NPs are shown in Figure 2. The number average diameter of Ni NPs measured from the TEM image is 41 nm. The PSD is

Table I. Formulations for the Synthesis of Metal Containing PAAm Particles by Inverse Miniemulsion Polymerization

Reagents (g)	R1	R2[a]	R3	R4[b]	R5[a]	R6[b]	R7	R8[b]
Continuous phase								
Isopar M	40.2	40.2	40.2	40.2	42.4	40.1	40.2	40.2
PE/B-*b*-PEO	0.30	0.30	0.30	0.30	0.30	0.40	0.30	0.30
Disperse phase								
DMSO	6.00	6.00	6.00	6.00	6.00	6.00	6.00	6.00
Ni		0.30		0.30	0.30	0.30		0.30
AAm	3.00	3.00	3.00	3.00	3.00	3.00	3.00	3.00
Brij 76	0.126	0.126	0.126	0.126	0.126	0.126	0.126	0.126
$NaNO_3$							0.708	0.708
$Zn(NO_3)_2.6H_20$			0.708	0.708	1.244	0.708		
$Ni(NO_3)_2.6H_20$	0.708	0.708						
Initial initiator solution								
AIBN	0.120	0.120	0.120	0.120	0.120	0.120	0.120	0.120
Toluene	2.40	2.40	2.40	2.40	2.40	2.40	2.40	2.40

[a]Additional initiator solution (0.060 g AIBN in 1.20 g of toluene) added after 4 h of reaction.
[b]Additional initiator solution (0.120 g AIBN in 2.40 g of toluene) added after 4 h of reaction.

relatively broad (PDI = 1.7) with particle sizes ranging from 20 nm to 120 nm.

Three different polar solvents, such as water, ethanol, and DMSO, and five different surfactants, i.e. the non-ionic Brij 76, Lutensol AT11, Lutensol AT50, Tween 80, and the anionic SDS were employed to disperse the Ni NPs. When either water or ethanol was used as polar solvent to disperse the Ni NPs with any of the five tested surfactants, Ni NPs started to precipitate right after sonication. However, when DMSO was used as polar solvent with surfactant Brij 76 to stabilize Ni NPs, no precipitate could be observed. This result may be attributed to the higher viscosity, density, and dipolar moment of DMSO, compared to water and ethanol, as shown in Table II.[24]

Inverse AAm Miniemulsion Polymerization

The stability of inverse miniemulsions is enhanced by using a combination of an effective surfactant and an osmotic pressure agent (lipophobe), which has a very low solubility in the lipophilic continuous phase and, thus, prevents Ostwald ripening.[17] Furthermore, beside the control of the osmotic pressure in the droplets, the lipophobe can also influence the interfacial properties of the disperse and continuous phases.[18,19] They can interact with the other compounds in the disperse phase including monomer and surfactant. In addition, the composition of the organic phase and dissociation of salts as a function of the salt nature are also very important regarding the properties of the final particles and colloidal stability of the system.[25]

To evaluate the effect of different lipophobes on the particle formation via inverse miniemulsion polymerization, different kinds of salts were used in the blank reactions (without Ni NPs): two cations of transition metals (Zn^{+2}, Ni^{+2}), one alkali metal cation (Na^{+}), and one anion (NO_3^{-}), as presented in Table I. Reaction R1 with nickel salt conducted with a similar mol% of lipophobe as reaction R3 with zinc salt, resulted in the formation of the smallest particles with Dp_n = 214 nm (Table III and Figure 3). This could be explained by the increase of the ion concentration in the droplets, which favors the suppression of molecular diffusion due to the building of an osmotic pressure

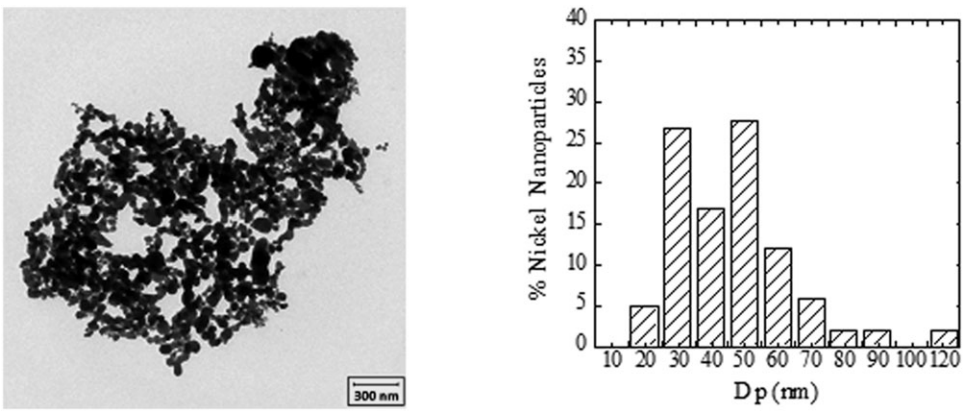

Figure 2. TEM image (left) and particle size distribution (right) of nickel nanoparticles.

Table II. Physical Properties of Polar Solvents at 25°C[24]

Solvent	Molecular structure	Viscosity (cP)	Density (g cm^{-3})	Dipole moment
Water	H_2O	0.890	0.997	1.85 D
Ethanol	C_2H_6O	1.074	0.789[a]	1.69 D
DMSO	C_2H_6OS	1.987	1.101	3.96 D

[a]Density of ethanol at 20°C.

Table III. Average Particle Size of PAAm Particles Prepared by Inverse Miniemulsion (Blank Reactions Without Ni NPs)

Reaction	Lipophobe type	Lipophobe (mol %)[a]	Dp_n (nm)	Dp_w (nm)	PDI
R3	$Zn(NO_3)_2{\cdot}6H_20$	5.3	302	363	1.20
R1	$Ni(NO_3)_2{\cdot}6H_20$	5.4	214	293	1.37
R7	$NaNO_3$	16.5	439	453	1.03

[a]Based on monomer.

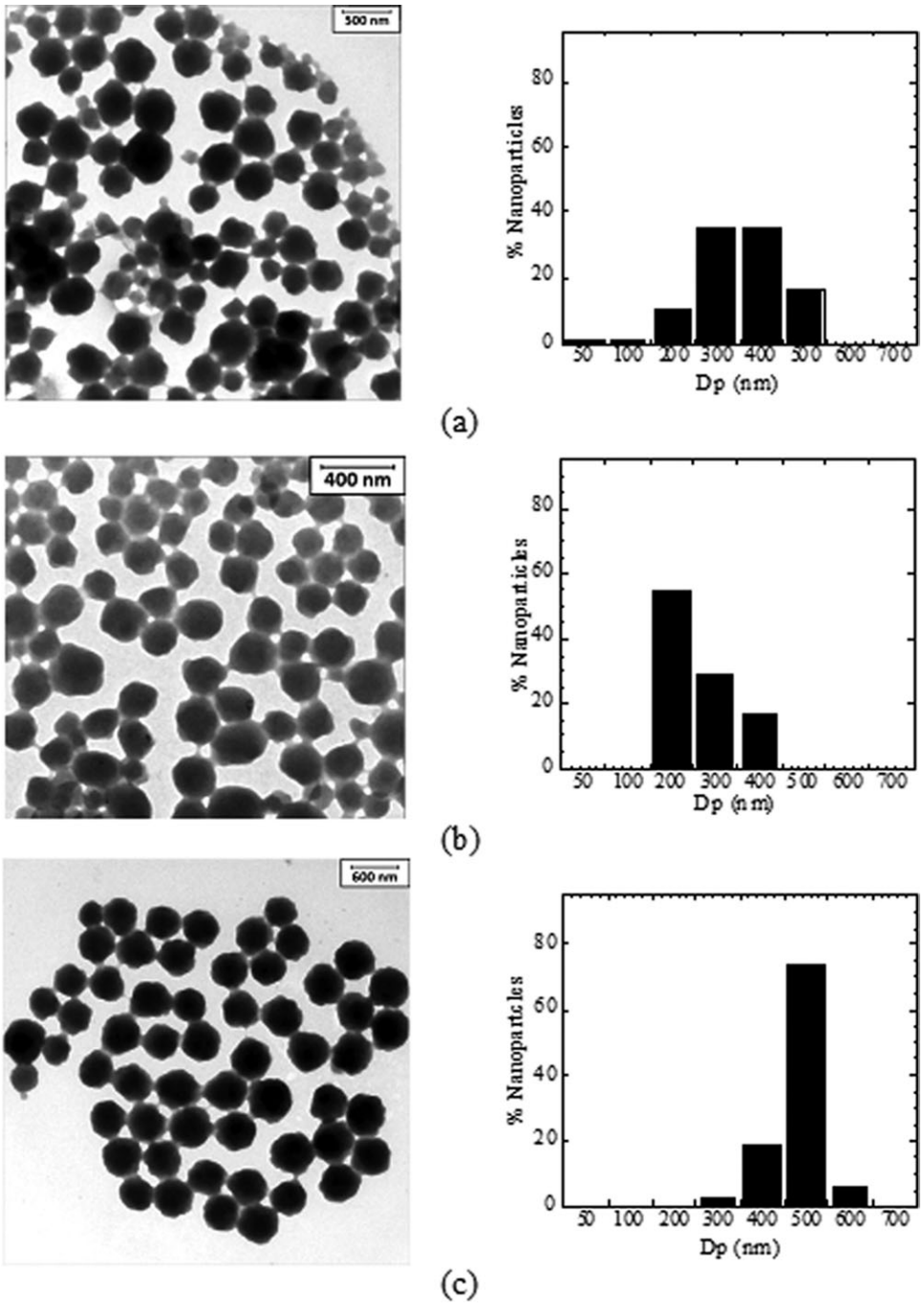

Figure 3. TEM images (left) and size distributions (right) of blank PAAm particles synthesized with different lipophobes: (a) R3 with $Zn(NO_3)_2{\cdot}6H_20$, (b) R1 with $Ni(NO_3)_2{\cdot}6H_20$, and (c) R7 with $NaNO_3$.

Table IV. Average Particle Size of PAAm Particles with Encapsulated Ni NPs Prepared by Inverse Miniemulsion with Different Lipophobes

Reaction	Lipophobe type	Lipophobe (mol %)[a]	Dp_n (nm)	Dp_w (nm)	PDI
R4	$Zn(NO_3)_2{\cdot}6H_20$	5.3	299	450	1.51
R2	$Ni(NO_3)_2{\cdot}6H_20$	5.4	419	485	1.16
R8	$NaNO_3$	16.5	508	1105	2.03

[a]Based on monomer.

that counteracts the Laplace pressure on the droplets.[19] Therefore, smaller particles with a low PDI were obtained with the Ni salt, indicating that the dissociation ability of $Ni(NO_3)_2$ in mixtures of DMSO, water, and AAm is higher when compared to $Zn(NO_3)$.

The ionic strength on a concentration basis is given by $I = 1/2 \sum_{i=1}^{n} c_i z_i^2$ where c_i and z_i are, respectively the molar concentration and charge number of ion *i*. Therefore, when nickel and zinc salts were replaced by a sodium salt in reaction R7, the

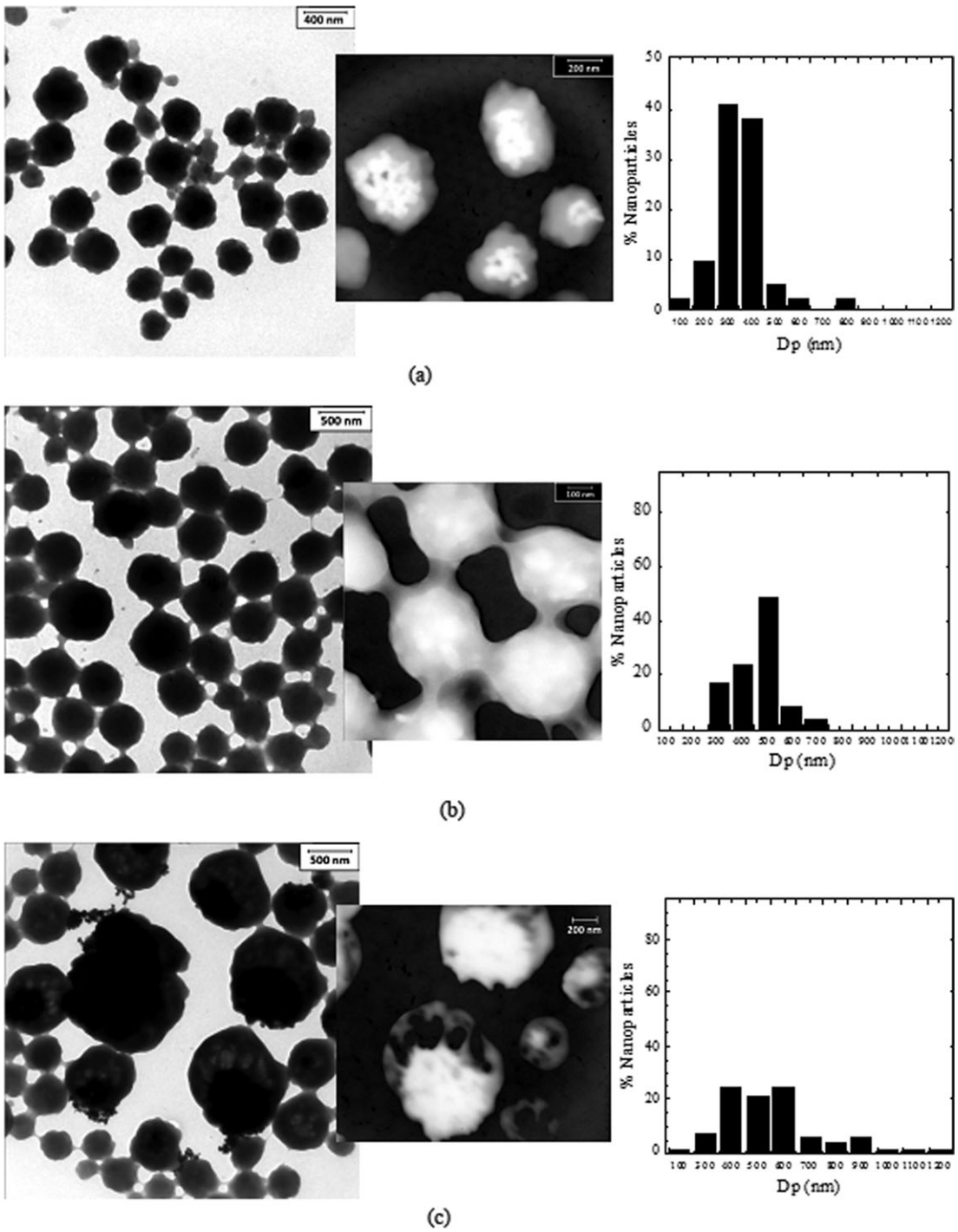

Figure 4. TEM images (left) and particle size distributions (right) of PAAm particles with incorporated Ni NPs, which were synthesized with different types of lipophobe: (a) R4 ($Zn(NO_3)_2{\cdot}6H_2O$), (b) R2 ($Ni(NO_3)_2{\cdot}6H_2O$), (c) R8 ($NaNO_3$).

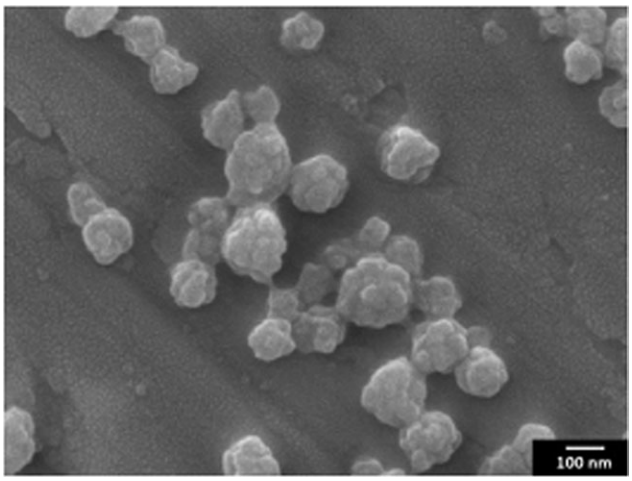

Figure 5. FEG-SEM images of Ni containing PAAm particles synthesized in the presence of $Ni(NO_3)_2{\cdot}6H_20$ as lipophobe (sample R2).

amount of sodium salt ($NaNO_3$) in moles at the same mass of the salts was approximately three times higher than that of nickel and zinc salts [$Ni(NO_3)_2$ and $Zn(NO_3)_2$] in order to provide a similar ionic strength. As shown in Table III and Figure 3, reaction R7 resulted in the largest particle size (Dp_n = 439 nm) with the narrowest particle size distribution (PDI = 1.03).

Encapsulation of Nickel Nanoparticles by Inverse AAm Miniemulsion Polymerization

Reactions with Different Types of Lipophobes. In the inverse miniemulsion polymerization systems containing Ni NPs, the smallest number average diameter (300 nm) was obtained when $Zn(NO_3)_2{\cdot}6H_2O$ was used as lipophobe (see Table IV). In addition, comparing the average particle sizes of PAAm particles with 10 wt % of Ni NPs (Table IV) with those of the respective blank reactions (Table III) it could be seen that the incorporation of Ni NPs leads to a systematic increase of the average particle size for all tested lipophobes. This increase results from the tendency of magnetic particles to agglomerate resulting in larger polymer particles.[20] It could be seen in TEM images [Figure 4 (a,b)] Ni NPs slightly aggregated within polymer particles. The Ni NPs can be identified as the bright white spots in the inverted TEM images caused by the higher electronic density of nickel compared to the polymer. In addition, latex particles seem to show a multilobe morphology.

After polymerization of AAm in the presence of Ni NPs and using $NaNO_3$ as lipophobe (sample R8) a huge increase in the particle's size polydispersity was observed in comparison to that of blank reaction R7 without Ni NPs (Table III). In addition, as it may be observed in the TEM image [Figure 4(c)], Ni NPs are not homogeneously distributed within the particles nor in the

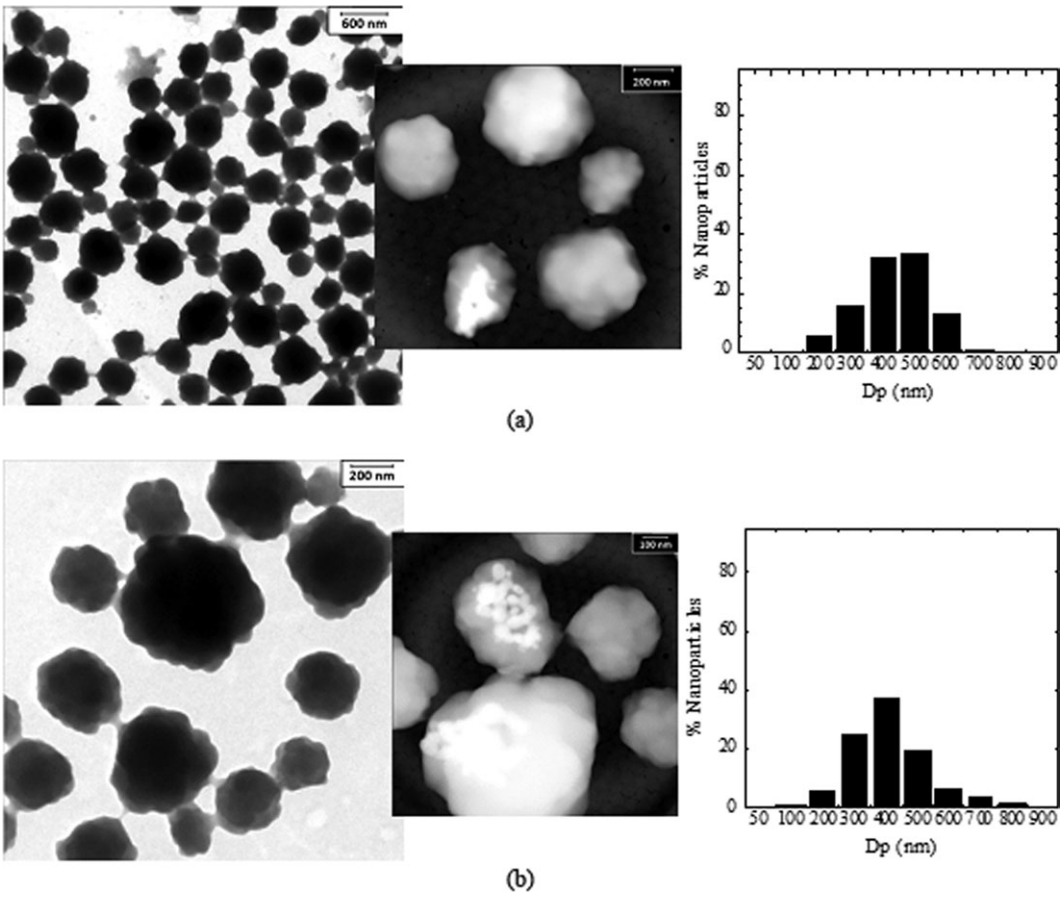

Figure 6. TEM images (left) and particle size distributions (right) of PAAm particles with incorporated Ni NPs and with $Zn(NO_3)_2{\cdot}6H_20$ used as lipophobe: (a) R5 and (b) R6.

Table V. Average Size of PAAm Particles Containing Ni NPs, Prepared by the Inverse Miniemulsion with $Zn(NO_3)_2{\cdot}6H_2O$ as Lipophobe

Reaction	$Zn(NO_3)_2{\cdot}6H_2O$ (mol %)[a]	PE/B-*b*-PEO (mol %)[a]	Dp_n (nm)	Dp_w (nm)	PDI
R4	5.3	10.0	299	450	1.51
R5	9.1	10.0	386	456	1.18
R6	5.3	13.3	384	505	1.32

[a]Based on monomer.

center, but concentrated at one side of the particle assuming a Janus-like morphology with pure PAAm on one side of the particles and Ni NPs displaced towards the opposite side and with some of the Ni NPs. This morphology was not observed in the case when either zinc or nickel salts were used as lipophobe [Figures 4(a,b), sample R4 or R2, respectively]. The concentration of Ni NPs near the surface of the PAAm particles in reaction R8 could possibly be attributed to the high molar concentration of $NaNO_3$, which was used in this reaction (as shown in Table IV). The TEM image inserted in Figure 4(c) was made after long electron beam exposure time and thus it may be observed that PAAm starts to degrade.

To assess the semi-quantitative and qualitative chemical composition of the hybrid particles, an energy dispersive system microprobe was used, which was coupled with the field emission gun Scanning electron microscope (FEG-SEM). Figure 5 shows a FEG-SEM image of sample R2, confirming the multilobe morphology of the particles. The punctual analysis of several particles resulted in 9.9 wt % of Ni in relation to the total solids. This value is in accordance with the amount of nickel added in the formulation (9.6 wt %, taking the amount of Ni present in the Ni salt into account).

Reactions with $Zn(NO_3)_2{\cdot}6H_2O$ as Lipophobe

The influence of the lipophobe content on the characteristics of PAAm particles with incorporated Ni NPs was examined using higher zinc salt concentrations (sample R5). In the TEM image Figure 6(a) it can be seen that the Ni NPs were encapsulated in PAAm particles and that the particle size distribution became narrower with increasing concentration of zinc nitrate hexahydrate from 5.3 to 9.1 mol % (in relation to acrylamide) with an increase of the average number diameter (Table V). Similar results were observed for the increase of zinc salt to the aqueous phase of a AAm inverse miniemulsion polymerization.[18] The authors credited the narrowing particle size distribution with increasing salt content to the decrease of the interfacial tension.[26]

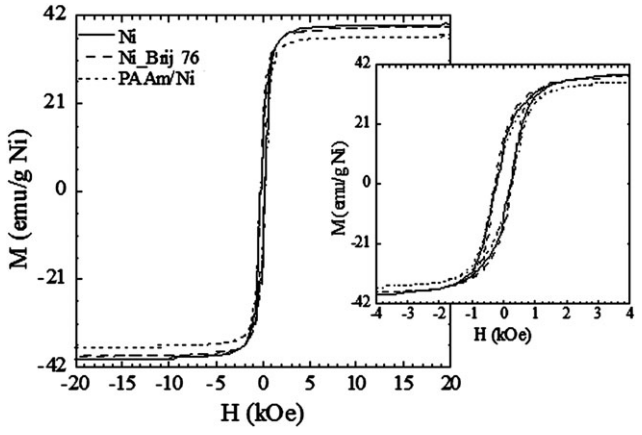

Figure 7. Magnetic field dependent magnetization curves of pure Ni NPs, Ni NPs stabilized with Brij 76 and PAAm/Ni particles (R4).

The increase of the surfactant concentration (PE/B-*b*-PEO) from 10.0 wt % to 13.3 wt % in relation to acrylamide in reaction R6 (Table V) did not result in a decrease of the particle size as compared to reaction R4. This behavior could eventually be attributed to the encapsulation of high amounts of Ni NPs aggregates, which may be observed in the inverted TEM image in Figure 6(b).

Magnetic Properties of Polymeric Particles

The magnetic properties of Ni NPs and PAAm/Ni particles were characterized by a vibrating sample magnetometer (VSM) at 300 K, for maximum field of 2 T. According to the magnetization curves shown in Figure 7 the saturation magnetization of pure Ni NPs, Brij 76 stabilized Ni NPs and PAAm/Ni particles prepared in reaction R4 are 40 emu/g Ni, 39 emu/g Ni, and 37 emu/g Ni, respectively. These results indicate that after encapsulation of Ni NPs in the PAAm matrix the magnetization of Ni remains very similar to pure Ni.

In addition, the magnetization curves with hysteresis loops suggest that the systems are predominantly formed by particles having ferromagnetic characteristics with a minor contribution of superparamagnetic particles. This magnetic behavior agrees with the morphology of the Ni NPs observed in the TEM images (Figure 2). According to this image Ni NPs are irregular, isolated and with a particle size distribution between 20 and 120 nm. This particle size range indicates the predominant presence of magnetic NPs with multi-domains ($\geq$20 nm) in addition to a small fraction of mono-domain NPs ($\leq$20 nm), since the critical diameter reported for mono-domain face-centered Ni is 22.6 nm.[27]

CONCLUSIONS

The inverse miniemulsion polymerization technique showed to be very effective to synthesize magnetic polyacrylamide/Ni particles. Polyoxyethylene 10 stearyl ether (Brij 76) was found to be a good stabilizer for nickel nanoparticles in dimethyl sulfoxide (component of the disperse phase of the inverse miniemulsion). A block copolymer poly(ethylene-*co*-butylene)-*b*-poly(ethylene oxide) (PE/B-*b*-PEO) was used as surfactant and different types of salts, such as zinc, nickel, and sodium nitrates, were tested as lipophobe in the miniemulsion. Both salts resulted in the formation of hybrid particles having a multilobe morphology. Nickel nanoparticles can be identified in the TEM images due to the higher electronic density of nickel compared to the polymer. The increase of the concentration of zinc nitrate hexahydrate from 5.3 to 9.1 mol % (in relation to acrylamide) resulted in the formation of slightly larger particles with a narrow size distribution, but did not seem to affect the encapsulation yield of nickel nanoparticles. When high concentrations of sodium salt (16.5 mol % in relation to acrylamide) were used as lipophobe, nickel nanoparticles were found to be concentrated near

the outer surface of the polymer particles and/or expelled. Magnetization curves show that the used nickel nanoparticles have predominantly ferromagnetic properties and that the saturation magnetization of polyacrylamide/nickel particles is very similar to that of the pure nickel nanoparticles.

ACKNOWLEDGMENTS

The authors thank the financial support from CNPq — Conselho Nacional de Desenvolvimento Científico e Tecnológico, BMBF — Bundesministerium für Bildung und Forschung and PETROBRÁS and LCME (Laboratório Central de Microscopia Eletrônica) of UFSC (Universidade Federal de Santa Catarina) for the FEG-SEM analysis.

REFERENCES

1. Mahdavian, A. R.; Sehri, Y.; Mobarakeh, H. S. *Europ. Polym. J.* **2008**, *44*, 2482.
2. Schällibaum, J.; Dalla Torre, F. H.; Caseri, W. R.; Löffler, J. F. *Nanoscale* **2009**, *1*, 374.
3. Medeiros, S. F.; Santos, A. M.; Fessi, H.; Elaissari, A. *Intern. J. Pharm.* **2011**, *403*, 139.
4. Gong, C.; Duan, Y.; Tian, J.; Wu, Z.; Zhang, Z. *J. Appl. Polym. Sci.* **2008**, *110*, 569.
5. Roveimiab, Z.; Mahdavian, A. R.; Biazar, E.; Heidari, K. S. *J. Colloid Sci. Biotechnol.* **2012**, *1*, 82.
6. Rahman, M. M.; Elaissari, A. *J. Colloid Sci. Biotechnol.* **2012**, *1*, 3.
7. Chou, K. S.; Huang, K. C.; Shih, Z. H. *J. Appl. Polym. Sci.* **2005**, *97*, 128.
8. Kim, S.; Yoo, B. K.; Chun, K.; Kang, W.; Choo, J.; Gong, M. S.; Joo, S. W. *J Molecular Cataly.* **2005**, *226*, 231.
9. Xu, P.; Han, X.; Wang, C.; Zhou, D.; Lu, Z.; Wen, A.; Wang, X.; Zhang, B. *J. Phys. Chem. B* **2008**, *112*, 10443.
10. Chen, R.; MacLaughlin, S.; Botton, G.; Zhu, S. *Polymer* **2009**, *50*, 4293.
11. Joumaa, N.; Toussay, P.; Lansalot, M.; Elaissari, A. *J. Polym. Sci.* **2008**, *46*, 327.
12. Lu, S.; Forcada, J. *J. Polym. Sci.: Part A: Polym. Chem.* **2006**, *44*, 4187.
13. Landfester, K.; Willert, M.; Antonietti, M. *Macromolecules* **2000**, *33*, 2370.
14. Qi, G.; Jones, C. W.; Schork, F. J. *Macromol. Rapid Commun.* **2007**, *28*, 1010.
15. Ouyang, L.; Wang, L.; Schork, F. J. *Macromol. React. Eng.* **2011**, *5*, 163.
16. Antonietti, M.; Landfester, K. *Prog. Polym. Sci.* **2002**, *27*, 689.
17. Capek, I. *Adv. Coll. Interf. Sci.* **2010**, *156*, 35.
18. Kobitskaya, E.; Ekinci, D.; Manzke, A.; Plettl, A.; Ziemann, P.; Ziener, U.; Landfester, K. *Macromolecules* **2010**, *43*, 3294.
19. Crespy, D.; Landfester, K. *Polymer* **2009**, *50*, 1616.
20. Xu, Z. Z.; Wang, C. C.; Yang, W. L.; Fu, S. K. *J. Magnet. Magn. Mat.* **2004**, *277*, 136.
21. Lin, C. L.; Chiu, W. Y.; Don, T. M. *J. Appl. Polym. Sci.* **2006**, *100*, 3987.
22. Medeiros, S. F.; Santos, A. M.; Fessi, H.; Elaissari, A. *J. Colloid Sci. Biotechnol.* **2012**, *1*, 99.
23. Thomas, A.; Schlaad, H.; Smarsly, B.; Antonietti, M. *Langmuir* **2003**, *19*, 4455.
24. "Laboratory Solvents and Other Liquid Reagents" in CRC Handbook of Chemistry and Physics, 92nd Edition (Internet Version 2012), W. M. Haynes, ed., CRC Press/Taylor and Francis, Boca Raton, FL.
25. Cao, Z.; Wang, Z.; Herrmann, C.; Landfester, K.; Ziener, U. *Langmuir* **2010**, *26*, 18008.
26. Ivanova, E.; Blagodatskikh, I.; Vasil'eva, O.; Barabanova, A.; Khokhlov, A. *Polym. Sci. Ser. A* **2008**, *50*, 9.
27. Guimarães, A. P. Principles of Nanomagnetism; Springer: Dordrecht, **2009**; Chapter 2, p 38.